On the Importance of Video Action Recognition for Visual Lipreading

Xinshuo Weng
Carnegie Mellon University
xinshuow@cs.cmu.edu

Abstract

We focus on the word-level visual lipreading, which requires to decode the word from the speaker's video. Recently, many state-of-the-art visual lipreading methods explore the end-to-end trainable deep models, involving the use of 2D convolutional networks (*e.g.*, ResNet) as the front-end visual feature extractor and the sequential model (e.g., Bi-LSTM or Bi-GRU) as the back-end. Although a deep 2D convolution neural network can provide informative image-based features, it ignores the temporal motion existing between the adjacent frames. In this work, we investigate the spatial-temporal capacity power of I3D [5] (Inflated 3D ConvNet) for visual lipreading. We demonstrate that, after pre-trained on the large-scale video action recognition dataset (*e.g.*, Kinetics), our models show a considerable improvement of performance on the task of lipreading. A comparison between a set of video model architectures and input data representation is also reported. Our extensive experiments on LRW [17] shows that a two-stream I3D model with RGB video and optical flow as the inputs achieves the state-of-the-art performance.

1 Introduction

Visual lipreading, the ability to decode what is being said from the visual information alone, is a very challenging task for both human and machine due to its ambiguity. As the McGurk effect introduced in [21], different characters can produce similar lip movement (e.g., 'p' and 'b'). These characters, called homophones, are difficult to be determined from visual cues alone. However, people have demonstrated that this ambiguity can be resolved to some extent using the context of neighboring characters (*i.e.*, word-level lipreading) or words (*i.e.*, sentence-level lipreading). In this work, we focus on the word-level visual lipreading. Specifically, we aim to compute the probability distribution over the words existing in the dictionary given a video in which a word is being said by the speaker.

People have traditionally approached the visual lipreading by a two-stage paradigm, including feature extraction from the mouth region and classification using the sequence model. The most common feature extraction approach is the use of a dimension reduction or compression method, with the most popular being the Discrete Cosine Transform (DCT) [45, 24, 29, 28]. This gives us a compact image based features of the mouth for each frame. In the second stage, a sequence model, such as Hidden Markov Models (HMMs) [35, 32, 8], is used to model the temporal information existing in the extracted image based features.

Recently, many deep learning approaches for lipreading [43, 17, 41, 27, 23, 39, 2, 22, 36, 26] has been proposed and achieve the state-of-the-art performance, in which the two-stage paradigm is replaced by the end-to-end trainable neural networks with a front-end feature extractor and a back-end recurrent neural network. Similar to the traditional methods, high dimension videos of cropped mouth is fed into the front-end and thus a compact and informative features are extracted. The extracted features are then passed through the back-end model for classification. As the gradient computed from the cross entropy loss can be pass from the back-end to the front-end, the overall neural network is end-to-end trainable. Often times, people use a deep 2D convolutional neural network (CNNs),

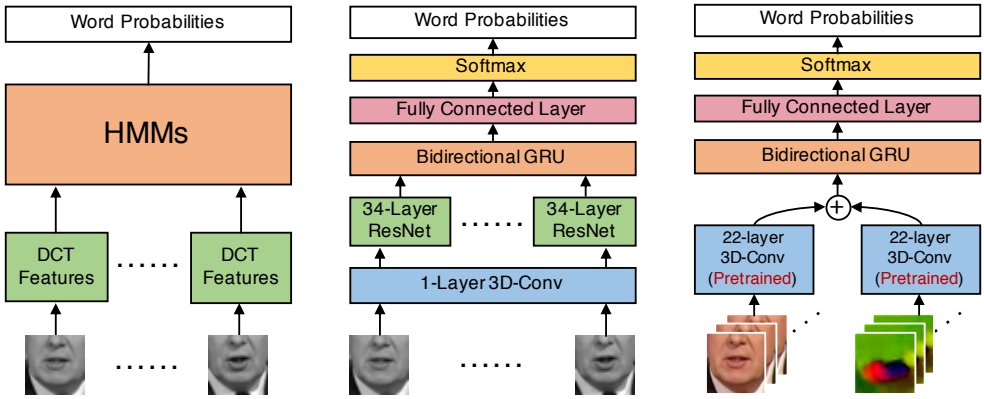

(a) (b) (c)

Figure 1: Illustration of model paradigm for traditional two-stage methods (a), recent deep learning based methods (b) and our proposed method. The major difference is that the previous works only explore the strong 2D image-based features (or the 3D features extracted from a shallow 3D CNN) for visual lipreading, while our method succeeds by investigating the spatial-temporal capacity power of the deep 3D CNNs for visual lipreading.

such as ResNet [12], or a shallow 3D CNN plus a deep 2D CNN, as the front-end to extract image based features independently from each frame and a bi-directional recurrent neural network, such as Bi-GRU, Bi-LSTM, as the back-end.

However, it is commonly accepted that image based deep features extracted from 2D CNNs are not directly suitable for video task (*e.g.*, lipreading) due to the lack of motion modeling. Intuitively, it is more natural to use the deep 3D CNNs as the front-end to extract the spatial-temporal features before feeding into the back-end models. Surprisingly, only a few works [3, 41, 1, 27], to the best of our knowledge, have explored the use of 3D CNNs for lipreading. Also, only shallow 3D CNNs (*e.g.,* one-layer or three-layers) are used in those works, in which the network architecture design is contradictory to our common knowledge that a deep neural network is expected to do better than a shallow one on a large-scale dataset. In our experiments, we show that it is actually the deep 2D CNN part instead of the shallow 3D CNN part makes the major contributions in previous works. Also, directly training a deep 3D CNN often leads to poor performance due to overfitting.

In this paper, we present the first successful deep end-to-end 3D CNN for visual lipreading. We illustrate the difference of the model paradigm between our method with the aforementioned two category methods in Figure 1. To the best of our knowledge, this is the first work to investigate the spatial-temporal capacity power of deep 3D CNNs beyond three layers for lipreading. Specifically, we use a 3D version of 22-layer Inception-v1 network [38] as our front-end. One common issue is that the deep 3D CNNs are much harder to train than their 2D counterparts because they have additional kernel dimension and seem to preclude the benefits of ImageNet pre-training. To handle this issue, we borrow the idea from I3D [5], first proposed for video action recognition, by inflating the pre-trained weights of the 2D Incetion-v1 network on ImageNet into three dimensions as the initialization for 3D kernels. With the conclusion from [10], when pre-trained on the large-scale video datasets, a 3D CNN can eventually achieve better performance on other video datasets after fine-tuning, we do a second round pre-training of our 3D CNN on Kinetics [5], which is a large-scale video action recognition dataset. We observe a similar behavior of performance improvement on lipreading dataset LRW [17].

Upon our pre-training strategy for our front-end I3D, We also investigate different combinations of video model architectures and input data representation (Grayscale, RGB, optical flow) for lipreading. We show that the back-end Bi-GRU model is still necessary even when we have a deep 3D CNN as our front-end. On the other hand, although a deep 3D CNN should be able to learn spatial-temporal features from RGB/Grayscale inputs directly, we empirically found that using optical flow as an additional input to represent the motion directly is still beneficial. Our extensive experiments on LRW shows that a pre-trained two stream I3D model with RGB video and optical flow as the inputs achieves the state-of-the-art performance.

Our contributions are three-fold: (1) it is the first work to investigate the spatial-temporal capacity power of deep 3D CNNs beyond three layers for lipreading; (2) we show that the two-round pre-training on large-scale datasets leads to much better local minimum when training the deep 3D CNN and avoids the overfitting; (3) we empirically found that using optical flow is beneficial for lipreading, and thus the two-stream deep I3D model with RGB video and optical flow as the inputs is the best performing model among proposed models and also achieve the state-of-the-art result on LRW.

2 Related Work

Visual Lipreading. Existing methods to approach lipreading by using visual information alone can be mostly split into two categories. The first traditional category method is mainly composed of separate two stages process involving a front-end and a back-end, as shown in Figure 1a. In the first stage, the spatial features are extracted from the cropped mouth region independently for each frame by using unsupervised feature extractors (*e.g.*, DCT). Then, a sequential model (*e.g.*, HMM) is applied on top of the extracted features to aggregate temporal information for classification.

Different variants of this category method can happen when people have a different combination of data pre-processing, feature extractors and sequential models as the classifier. [24] proposes a DCT coefficient selection procedure, which prefers more higher-order vertical components of the DCT coefficients, to achieve better performance when the variety of the hand pose is large in the dataset. [29] proposes a new cascaded feature extraction process including not only DCT but also a linear discriminant data projection and a maximum likelihood-based data rotation. [45] proposes a PCA based method to reduce the dimension of DCT based features. However, by separating out the feature extraction process from training the classifier in these traditional methods, the extracted features might not be the best suitable features for classification.

The second category methods approach the visual lipreading based on the recent advance of deep learning methods. The major difference is that there is no longer separate two stages for front-end feature extraction and back-end classification. The entire system including the front-end and back-end is trained end-to-end and thus the front-end feature extraction process is more class-dependent.

The variants of this category methods often differ from the architecture design of the front-end and back-end neural network modules. [23] is the first work to propose to use CNN in the front-end for feature extraction beyond using offline feature extractors in the conventional methods. [2] proposes a speaker-adaptive training procedure to achieve speaker independent lipreading system with the use of deep neural networks. [43] proposes to use LSTM as the back-end for classification and shows a significant improvement over the traditional classifiers. [17] takes the advantage of proposed large-scale lipreading dataset and also proposes a VGG-like network in the front-end for lipreading. Furthermore, [41] leverage the more advanced 2D CNN architecture of ResNet into lipreading system. Beyond visual features, [27] propose to use CNN to extract audio features and then fuse with extracted visual features. However, existing methods in this category have only explored the space of deep 2D CNN for image-based feature extraction, which ignores the temporal motion between adjacent frames. Our proposed method also lies in this category. Instead of using deep 2D CNNs, our proposed model has a deep 3D CNN as the front-end which is more intuitive to extract features from video.

Architecture Design for Video Action Recognition. In video action recognition, it has been a long time that people have developed effective and efficient CNN architectures specifically for video. Most variants of video architectures can be summarized into five main categories shown in Figure 2, in which we have only seen that (a) is widely explored for lipreading as mentioned above. However, no spatial-temporal information is considered during the front-end stage in (a).

To model appearance and motion information simultaneously, [42, 16, 40] proposes to use 3D convolution operation in the neural network, shown in Figure 2 (b) and thus outperforms the 2D CNN features on various video analysis tasks. Moreover, beyond shallow 3D CNNs, [11, 9] explores the effectiveness of ResNet with 3D convolutional kernels. To avoid overfitting, [30] proposes to simplify the 3D convolutions with 2D filters on spatial dimension plus 1D temporal connections and obtain further improvement over 3D ResNet. On the other hand, as the optical flow representation can model the motion directly, [33, 9, 44] proposes to use the optical flow as the inputs to compensate the disadvantage of 2D CNNs in video tasks, shown in Figure 2 (c). As the natural combination of using two stream networks and deep 3D CNN, [20, 5] proposes to train a two-stream 3D CNN for

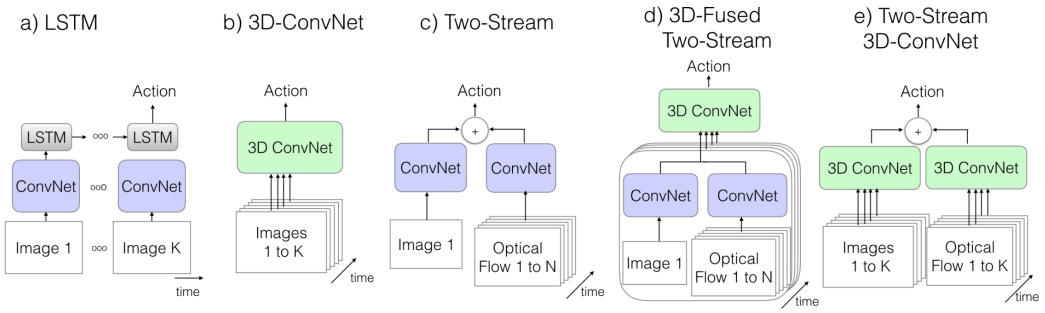

Figure 2: Successful video architectures developed for video action recognition. (a) LSTM is applied on top of extracted 2D image-based features; (b) 3D CNN is used to learn spatial-temporal representation directly from videos; (c) Optical flow is used to model the direct motion within a two-stream networks; (d)(e) Optical flow and 3D CNNs are both used in the two-stream network to model motion from different aspects.

action recognition, shown in Figure 2 (d)(e). In this paper, we aim to replicate the success happened in video action recognition to the task of visual lipreading.

3 Video Architectures for Visual Lipreading

In this section, we explore different strategies and model selections for visual lipreading. In summary, we adopt a hierarchical deep learning framework. For each video, our framework aims to predict the most likely word within the vocabulary; therefore our target could be considered as a multiclass classification problem.

3.1 Architecture Framework

In Figure 3, we decompose our framework of architecture for visual lipreading as follows: (a) inputs might be a sequence of grayscale images, RGB images, optical flow data, or the combination of them, depending on which following models are used; (b) a front-end module is used to extract the features from the inputs; (c) a back-end module is used to aggregate the temporal information after the front-end and summarize the extracted features into a single vector which represents the scores for each word; (d) finally a softmax layer is applied to compute the probabilities for each word.

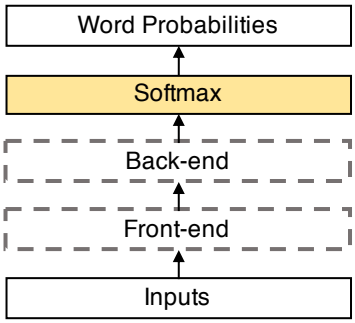

Figure 3: The architecture framework in this paper

The front-end and the back-end modules are not specified at this moment, but are placeholders for the modules to be introduced in following sections and can be replaced by them. We could see different performances with use of different combinations of the front-end and back-end modules.

3.2 Front-End Modules

We explore our front-end models progressively, where the most sophisticated model takes the advantage of the previous models. However, we separately introduce the ideas used for front-ends to show their intuitions. Figure 4 shows the evolution of front-ends introduced in this paper.

3.2.1 Recap: Shallow 3D ConvNet + Deep 2D ConvNet

As well-developed 2D deep CNNs have shown their strong capability in many image-based tasks [38, 12, 19, 34], [41] applies the very successful 2D CNN – ResNet for visual lipreading, which is also the baseline model to be compared in this paper. The deep 2D CNNs can extract features independently from each frame and then a sequential model, such as RNNs, to process the long

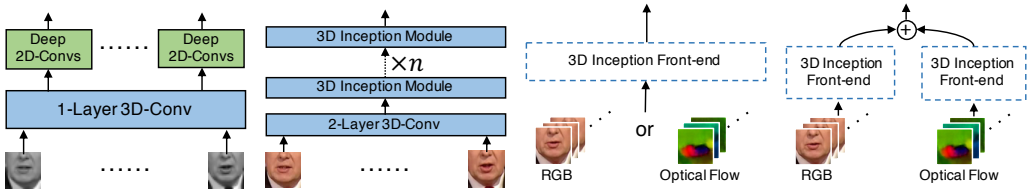

Figure 4: Illustration of front-end model paradigm for shallow 3D ConvNet + deep 2D ConvNet (a), deep 3D InceptionNet (b), one-stream front-end (c), two-stream deep 3D InceptionNet (d). These models evolve progressively, where the later models adopt the ideas of previous models.

dependencies and do prediction with those time frame features, which is in the spirit of many natural language processing works. However, since visual lipreading is a video task, which means the temporal relationship among pixels and 2D features are discarded with only 2D feature extracters, they propose to use 3D CNNs hierarchically before the deep 2D CNNs to utilize the short-term temporal relationships. In detail, they take grayscale images as input and pass it through one-layer 3D CNNs with 64 kernels of 5×7×7 (`time`×`width`×`height`, we keep this order in the following descriptions) kernel size, following with batch normalization [14] and ReLU activation (always applied if not specified, and do not reply it in the following sections), and the 3D features are then processed by ResNet on each time frame. Figure 4a illustrates the architecture of this model.

3.2.2 Deep 3D InceptionNet

Although [41] propose to use 3D CNNs to capture the temporal features, however, comparing to the much deeper 2D CNNs, the effect of the shallow 3D CNNs might be trivial. Also the temporal relationships might be discarded by the following 2D CNNs. Therefore, it is intuitive to use deep 3D CNNs alone to obtain the temporal features.

As the intuition of applying well-designed deep architectures, we also follow this setup by using the 22-layers 3D InceptionNet [5]. The 3D InceptionNet is similar to the original InceptionNet [14], but uses 3D CNNs instead of 2D CNNs. Figure 5 illustrates the detailed architecture of inception module.

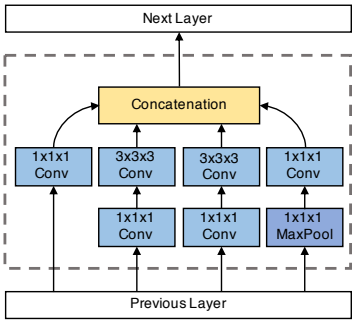

Figure 5: The structure of a single 3D Inception module. The stride size for the convolution and pooling operation is 1.

Figure 4b shows the architecture of the deep 3D model we adopt. We first use one layer of 3D convolution with 64 kernels of 7×7×7 kernel size and stride size 2 followed by a max-pooling layer of kernel size 1×3×3 and stride size 1×2×2, then we use another layer of 3D CNNs with 64 kernels of 3×3×3 and a max-pooling layer with the same parameters as the previous one. Then the following is a series of Inception modules and max-pooling layers.

3.2.3 Two-Stream Deep 3D InceptionNet

In theory, the deep 3D CNNs are expected to extract temporal features from direct image inputs, either grayscale or RGB, we expect better performance if we could incorporate direct motion in the inputs. Optical flow has shown its powerful effect in many video tasks [33, 4, 15] as a kind of core feature in computer vision. Optical flow captures the motion of pixels in neighboring images, and the representation of optical flow is the "speed" vector of each pixel. In this project, we use PWC-Net proposed by [37] to compute optical flow, and Figure 6 shows some computed optical flow examples, where we can observe that the pixels around the mouth are mostly highlighted.

Figure 6: Visualization examples of optical flow.

We explore three input setups in this paper: using single-stream with RGB inputs, using single-stream with optical flow inputs, and using two-stream inputs of RGB images and optical flow. Figure 4c

presents the first two strategies and Figure 4d illustrate the two-stream strategy. In the two-stream strategy, two deep 3D front-ends are applied on the two input streams separately, and the features are combined with simple addition.

3.3 Back-End Modules

The front-end models are supposed to reduce the dimension from time, width, and height to time (plus the feature dimension), and the back-end model would infer the scores for the words using the feature sequence.

3.3.1 Temporal ConvNets

Just like typical image classification tasks, we could use only convolution networks for classification. The difference is that we would apply convolution on the temporal dimension. This is similar to the sentence classification with CNNs idea [18] which is widely used in natural language processing.

In this project, we use two layers of 1D temporal convolution networks followed by a linear layer to predict the scores for each word. The first CNN layer has 512 kernels of kernel size 5 and stride size 2, followed by max-pooling with kernel size 2 and stride size 2 and another CNN layer with 1024 kernels of the same kernel size as the first one.

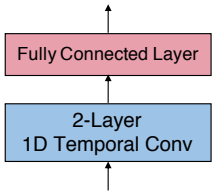

Figure 7: Temporal ConvNets back-end.

3.3.2 Bidirectional GRU

Another strategy is to apply typical sequential models as the back-end model, such as RNNs. Gated Recurrent Unit (GRU) [6] is developed as an extension of RNN and has fewer parameters than LSTM [13] while having similar performance. GRU can capture the long dependencies in sequences and prevent gradient exploding and vanishing just like LSTM. Bidirectional RNNs [31] is a widely adopted technique to improve the capability of RNNs in dealing with sequence problems like natural languages, since the cue of previous states may appear temporally later or vice versa.

Figure 8 shows the architecture of Bi-GRU back-end. We apply two-layer bidirectional GRUs on the temporal features, and pass the average of the last layer outputs through a linear layer to compute the word scores. The hidden state dimension in our implementation is 512.

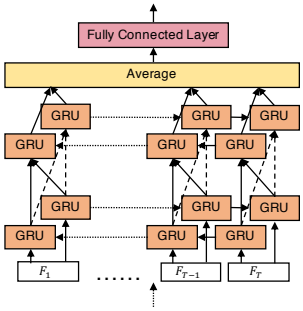

Figure 8: Two-layer bidirectional GRU back-end.

4 Two-Round Pre-training

Similar to the nature of using ImageNet pre-trained weights for 2D image-based tasks, we want to initialize the weights of our deep 3D CNNs in a proper way such that the optimization is easier and tends to not be overfitting. However, it is not possible to directly use the ImageNet pre-trained weights to initialize the 3D CNN kernels as the 3D convolution has an additional dimension of weights. Therefore, we follow the same strategy of initializing the 3D CNNs proposed by [5], which inflates the ImageNet pre-trained weights into three dimensions by repeating the weights of the 2D filters N times along the time dimension.

However, repeating the ImageNet pre-training weights can only make the initialized 3D kernels to be able to extract spatial features independently for each channel. As demonstrated in [5, 10], when pre-trained on the large-scale video datasets, a deep 3D CNN can eventually achieve better performance on other video datasets after finetuning. We thus have a second-round pre-training on the large-scale video dataset – Kinetics [5] such that our initialized 3D kernels can be directly suitable for extracting spatial-temporal features when finetuning on the LRW dataset.

5 Dataset

We train and evaluate our proposed models on the word-level lipreading dataset LRW [17]. The dataset consists of short clips of videos (488,766 for training, 25,000 for validation and 25,000 for testing) extracted from BBC TV broadcasts (News, Talk Shows, etc.). There are 29 frames of RGB images for each video sequence. LRW dataset is characterized by its high variability with respect to speakers and pose. Moreover, the number of target words is 500, which is an order of magnitude higher than other publicly available databases (GRID [7], CUAVE [25], etc.). The other feature is the existence of pairs of words that share most of their visemes. Such examples are nouns in both singular and plural forms (e.g. benefit-benefits, 23 pairs) as well as verbs in both present and past tenses (e.g. allow-allowed, 4 pairs). Perhaps the most difficult part of the dataset is the fact that the target words appear within utterances rather than being isolated. Hence, the network should learn not merely how to discriminate between 500 target words, but also how to ignore the irrelevant parts of the utterance and spot one of the target words. And it should learn how to do so without knowing the word boundaries.

6 Data Pre-Processing and Augmentation

6.1 Cropping the Mouth Region

Figure 9: Random sequences of cropped mouth and their corresponding labels from LRW.

As the original sequences of images contain the entire faces of the speakers and the surrounding background, which are the irrelevant contexts for identifying the spoken words, we follow the conventional rules of cropping the mouth region from the original sequences using a fixed bounding box with the size of 96×96. Therefore, we end up with $96 \times 96 \times 29 \times 3$ RGB or $96 \times 96 \times 29$ grayscale video data for each sequence. The cropped videos are roughly centered at the mouth as the original videos in the datasets are already centered. Some random sequences of cropped mouth and their corresponding labels from LRW are shown in Figure 9.

6.2 Generating the Optical Flow

The dense optical flow is obtained by using the open-source code of PWC-Net [37]. For each pair of images in the sequence, we compute the corresponding flow with the size of $96 \times 96 \times 2$, representing the flow map along x and y dimension respectively. We then stack the flow map over the entire sequence and end up with $96 \times 96 \times 28 \times 2$ optical flow video data for each sequence.

6.3 Data Augmentation

We follow the conventional data augmentation mechanisms for the cropped mouth videos during training, including random horizontal flip, random cropping so that the sequences of images are not very well centered at the mouth, and normalization with respect to the overall mean and variance of the dataset. When using the two-stream networks, we augment the data in the same way for both two streams so that the data in two streams are well aligned spatially.

7 Experiments

In this section, we compare the performance of models with different combinations of front-end and back-end modules introduced in previous sections. As the word-level lipreading is a classification task, we evaluate the performance in all following sections using the classification accuracy based on the top-1 prediction on both the validation and testing dataset.

7.1 Evaluating the Back-End Modules

We first focus on the back-end modules of the network by comparing the Bi-GRU with the temporal convolution while fixing the front-end module as the baseline front-end (i.e., shallow 3D ConvNet +

Method	Val	Test
Shallow 3D + Deep 2D + Temporal Conv	68.79	68.55
Shallow 3D + Deep 2D + Bi-GRU	74.95	74.77

(a)

Method	Val	Test
Deep 2D + Bi-GRU	74.37	74.23
Shallow 3D + Deep 2D + Bi-GRU	74.95	74.77

(b)

Method	Val	Test
Shallow 3D + Deep 2D + Bi-GRU	74.95	74.77
Deep 3D InceptionNet + Bi-GRU	57.11	57.45
Deep 3D InceptionNet (Pre-Trained) + Bi-GRU	77.73	77.52

(c)

Method	Val	Test
RGB 3D InceptionNet (Pre-Trained) + Bi-GRU	77.73	77.52
Flow 3D InceptionNet (Pre-Trained) + Bi-GRU	78.17	77.93
Two-Stream 3D InceptionNet (Pre-Trained) + Bi-GRU	**82.11**	**82.07**

(d)

Table 1: Results on the LRW dataset.

Deep 2D ResNet). The results are shown in Table 1a. It shows a similar result as in [41] that using Bi-GRU is much better than a ConvNet in the back-end.

7.2 Evaluating the Effectiveness of Shallow 3D CNNs

As the existing baseline methods usually contain a shallow 3D CNN besides a deep 2D CNN in the front-end module, we want to see which part of the front-end modules in the baseline contributes the most to the final performance. We simply remove the shallow 3D CNN from the baseline while fixing the back-end module as the Bi-GRU. The results are shown in Table 1b. We can see that the performance does not drop much after removing the shallow 3D CNN in the front-end. This result demonstrates that the capacity power of a shallow 3D CNN is limited. The most useful information extracted in the features might come from the deep 2D CNN model, while the shallow 3D CNN does not help much.

7.3 Evaluating the Proposed Deep 3D InceptionNet and Two-Round Pre-Training Strategy

To evaluate the effectiveness of the proposed deep 3D InceptionNet, we replace the baseline front-end with the deep 3D InceptionNet while fixing the back-end as the Bi-GRU and train both models from scratch. The results are shown in Table 1c. Surprisingly, the performance of our 3D model is even lower than the baseline model. However, after using our proposed two-round pre-training strategy, our 3D model obtains a significant performance improvement and even perform better than the baseline. This result shows that training a deep 3D CNN is indeed much harder than a deep 2D CNN and tends to overfit the dataset. Also, a proper pre-training using the large-scale dataset can be very helpful, which eventually leads to a much better local minimum.

7.4 Evaluating the Two-Stream Deep 3D InceptionNet

To demonstrate if the two-stream configuration is also useful for lipreading, we compare our two-stream deep 3D InceptionNet with its single-stream counterpart, including the RGB single-stream and optical flow single-stream deep 3D InceptionNet. We fix the back-end module for all models as the Bi-GRU. The results are shown in Table 1d. We can see that the optical flow single-stream performs slightly better than the RGB single-stream, which confirms that the use of optical flow to model the direct motion is indeed beneficial. Moreover, the two-stream networks with both RGB and optical flow as the inputs performs the best among all proposed models. We thus hypothesize that there might be complementary information between the RGB and the optical flow modality.

8 Conclusion

In this paper, we propose the first work to investigate the spatial-temporal capacity power of deep 3D CNNs beyond three layers for lipreading. More specifically, we propose a two-stream 22-layers 3D InceptionNet front-end module and achieve the state-of-the-art results on LRW with the Bi-GRU as the back-end. In the meantime, We found that optimizing a deep 3D CNN is indeed very difficult, which might be one of the reasons why previous works prefer to use only a shallow 3D CNN in the front-end module. However, we also demonstrate that, with the proper two-round pre-training strategy, we can train the deep 3D CNN successfully and avoid the overfitting on LRW. Moreover,

the two-stream configuration with the use of optical flow as an additional input, which is commonly used in modern video action recognition, is also beneficial to visual lipreading.

References

[1] T. Afouras, J. S. Chung, A. Senior, O. Vinyals, and A. Zisserman. Deep Audio-Visual Speech Recognition. *arXiv*, 2018. 2

[2] I. Almajai, S. Cox, R. Harvey, and Y. Lan. Improved Speaker Independent Lip Reading Using Speaker Adaptive Training and Deep Neural Networks. *ICASSP*, 2016. 1, 3

[3] Y. M. Assael, B. Shillingford, S. Whiteson, and N. D. Freitas. LipNet: End-to-End Sentence-Level Lipreading. *arXiv*, 2017. 2

[4] N. Bonneel, J. Tompkin, K. Sunkavalli, D. Sun, S. Paris, and H. Pfister. Blind video temporal consistency. *ACM SIGGRAPH*, 2015. 5

[5] J. Carreira and A. Zisserman. Quo Vadis, Action Recognition? A New Model and the Kinetics Dataset. *CVPR*, 2017. 1, 2, 3, 5, 6

[6] K. Cho, B. Van Merriënboer, C. Gulcehre, D. Bahdanau, F. Bougares, H. Schwenk, and Y. Bengio. Learning phrase representations using rnn encoder-decoder for statistical machine translation. *EMNLP*, 2014. 6

[7] A. Czyzewski, B. Kostek, P. Bratoszewski, J. Kotus, and M. Szykulski. An Audio-Visual Corpus for Multimodal Automatic Speech Recognition. *Journal of Intelligent Information Systems*, 2017. 7

[8] V. Estellers, M. Gurban, and J.-P. Thiran. On Dynamic Stream Weighting for Audio-Visual Speech Recognition. *IEEE Transactions on Audio, Speech, and Language Processing*, 2012. 1

[9] C. Feichtenhofer, A. Pinz, and A. Zisserman. Convolutional Two-Stream Network Fusion for Video Action Recognition. *CVPR*, 2016. 3

[10] K. Hara, H. Kataoka, and Y. Satoh. Can Spatiotemporal 3D CNNs Retrace the History of 2D CNNs and ImageNet? *CVPR*, 2017. 2, 6

[11] K. Hara, H. Kataoka, and Y. Satoh. Learning Spatio-Temporal Features with 3D Residual Networks for Action Recognition. *ICCVW 2017*, 2018. 3

[12] K. He, X. Zhang, S. Ren, and J. Sun. Deep Residual Learning for Image Recognition. *CVPR*, 2016. 2, 4

[13] S. Hochreiter and J. Schmidhuber. Long short-term memory. *Neural Computation*, 1997. 6

[14] S. Ioffe and C. Szegedy. Batch Normalization: Accelerating Deep Network Training by Reducing Internal Covariate Shift. *ICML*, 2015. 5

[15] J. Janai, F. Güney, A. Behl, and A. Geiger. Computer vision for autonomous vehicles: Problems, datasets and state-of-the-art. *arXiv*, 2017. 5

[16] S. Ji, M. Yang, and K. Yu. 3D Convolutional Neural Networks for Human Action Recognition. *TPAMI*, 2013. 3

[17] A. Z. Joon Son Chung. Lip Reading in the Wild. *ECCV*, 2016. 1, 2, 3, 7

[18] Y. Kim. Convolutional neural networks for sentence classification. *EMNLP*, 2014. 6

[19] A. Krizhevsky, I. Sutskever, and G. E. Hinton. Imagenet classification with deep convolutional neural networks. In *NIPS*, 2012. 4

[20] K. Liu, W. Liu, C. Gan, M. Tan, and H. Ma. T-C3D : Temporal Convolutional 3D Network for Real-time Action Recognition. *AAAI*, 2018. 3

[21] H. McGurk and J. MacDonald. Hearing Lips and Seeing Voices. *Nature*, 1976. 1

[22] H. Ninomiya, N. Kitaoka, S. Tamura, Y. Iribe, and K. Takeda. Integration of Deep Bottleneck Features for Audio-Visual Speech Recognition. *INTERSPEECH*, 2015. 1

[23] K. Noda, Y. Yamaguchi, K. Nakadai, H. G. Okuno, and T. Ogata. Lipreading using Convolutional Neural Network. *INTERSPEECH*, 2014. 1, 3

[24] A. Pass, J. Zhang, and D. Stewart. An Investigation into Features for Multi-View Lipreading. *ICIP*, 2010. 1, 3

[25] E. Patterson, S. Gurbuz, Z. Tufekci, and J. Gowdy. CUAVE: A New Audio-Visual Database for Multimodal Human-Computer Interface Research. *ICASSP*, 2002. 7

[26] S. Petridis and M. Pantic. Deep Complementary Bottleneck Features for Visual Speech Recognition. *ICASSP*, 2016. 1

[27] S. Petridis, T. Stafylakis, P. Ma, F. Cai, G. Tzimiropoulos, and M. Pantic. End-to-End Audiovisual Speech Recognition. *arXiv*, 2018. 1, 2, 3

[28] G. Potamianos, C. Neti, G. Gravier, A. Garg, and A. W. Senior. Recent Advances in the Automatic Recognition of Audiovisual Speech. *Proceedings of the IEEE*, 2003. 1

[29] G. Potamianos, C. Neti, and G. Iyengar. A Cascade Visual Front End for Speaker Independent Automatic Speechreading. *International Journal of Speech Technology*, 2001. 1, 3

[30] Z. Qiu, T. Yao, and T. Mei. Learning Spatio-Temporal Representation with Pseudo-3D Residual Networks. *ICCV*, 2017. 3

[31] M. Schuster and K. K. Paliwal. Bidirectional recurrent neural networks. *IEEE Transactions on Signal Processing*, 1997. 6

[32] X. Shao and J. Barker. Stream Weight Estimation for Multistream Audio-Visual Speech Recognition in a Multispeaker Environment. *Speech Communication*, 2008. 1

[33] K. Simonyan and A. Zisserman. Two-Stream Convolutional Networks for Action Recognition in Videos. *NIPS*, 2014. 3, 5

[34] K. Simonyan and A. Zisserman. Very deep convolutional networks for large-scale image recognition. *ICLR*, 2015. 4

[35] D. Stewart, R. Seymour, A. Pass, and J. Ming. Robust Audio-Visual Speech Recognition under Noisy Audio-Video Conditions. *IEEE Transactions on Cybernetics*, 2014. 1

[36] C. Sui, M. Bennamoun, and R. Togneri. Listening With Your Eyes : Towards a Practical Visual Speech Recognition System Using Deep Boltzmann Machines. *ICCV*, 2015. 1

[37] D. Sun, X. Yang, M.-Y. Liu, and J. Kautz. PWC-Net: CNNs for Optical Flow Using Pyramid, Warping, and Cost Volume. *CVPR*, 2018. 5, 7

[38] C. Szegedy, W. Liu, Y. Jia, P. Sermanet, S. Reed, D. Anguelov, D. Erhan, V. Vanhoucke, and A. Rabinovich. Going Deeper with Convolutions. *CVPR*, 2015. 2, 4

[39] Y. Takashima, R. Aihara, T. Takiguchi, and Y. Ariki. Audio-Visual Speech Recognition Using Bimodal-Trained Bottleneck Features for a Person with Severe Hearing Loss. *INTERSPEECH*, 2016. 1

[40] G. W. Taylor, R. Fergus, Y. Lecun, and C. Bregler. Convolutional Learning of Spatio-Temporal Features. *ECCV*, 2010. 3

[41] G. T. Themos Stafylakis. Combining Residual Networks with LSTMs for Lipreading. *INTERSPEECH*, 2017. 1, 2, 3, 4, 5, 8

[42] D. Tran, L. Bourdev, R. Fergus, L. Torresani, and M. Paluri. Learning Spatiotemporal Features with 3D Convolutional Networks. *ICCV*, 2015. 3

[43] M. Wand, J. Koutník, and J. Schmidhuber. Lipreading with Long Short-Term Memory. *ICASSP*, 2016. 1, 3

[44] Z. Wu, Y.-g. Jiang, X. Wang, H. Ye, and X. Xue. Multi-Stream Multi-Class Fusion of Deep Networks for Video Classification. *ACMMM*, 2016. 3

[45] H. Xiaopeng, Y. Hongxun, W. Yuqi, and C. Rong. A PCA Based Visual DCT Feature Extraction Method for Lipreading. *International Conference on Intelligent Information Hiding and Multimedia Signal Processing*, 2006. 1, 3